CrossMark

RESEARCH PAPER

Seismic Performance of Different Types of Connections Between Steel Bracing and RC Frames

Mahmoud R. Maheri[1] · S. Yazdani[1]

Abstract In this paper, the seismic performance of three different types of connections between steel braces and concrete frames is assessed through numerical analyses. Two of the connection types are similar to the conventional diagonal steel brace–steel frame connections, while the third type is a new connection specifically designed for increased ductility. Results of previous experimental studies are first used to verify the accuracy of numerical models of the connections. The connections are then incorporated into brace–RC frame systems, and nonlinear cyclic analyses of the brace–frame assemblage are carried out. The response hysteresis loops of the frames are then used to evaluate such strength and performance parameters as capacity, stiffness, stiffness degradation, energy dissipation, equivalent damping ratio and ductility ratio for the frames. These parameters are then compared for the frames containing the three different types of connections. It is found that while the two conventional connections can perform effectively when the capacity and stiffness of the frame are of prime interest, the new connection enhances ductility and improves energy absorption capacity of the frame.

Keywords Reinforced concrete · Steel bracing · Connection · Seismic performance · Seismic retrofitting

✉ Mahmoud R. Maheri
maheri@shirazu.ac.ir

[1] Department of Civil Engineering, Shiraz University, Shiraz, Iran

1 Introduction

Steel bracing is the simplest and the most economical method to increase the resistance of a frame to lateral loads. Traditionally, steel bracing is used in steel structures. However, in recent years, steel bracing has also been applied to retrofitting of reinforced concrete frames. Increased architectural flexibility, speed and cost of application are amongst the parameters making bracing more attractive compared to shear wall for retrofitting purposes. The concept of using steel bracing in new RC constructions has also been the subject of some recent investigations.

Steel bracing of RC frames can be applied either externally or internally. In the external bracing, steel trusses or frames are attached to the frame's exterior (Bush et al. 1991; Badoux and Jirsa 1990). In the internal bracing, steel bracing members are inserted inside the individual unit frames concurrent with the frames' axis. In this method, the steel braces can be connected to the RC frames either directly or indirectly. Earlier forms of internal bracing used intermediary steel frames inside the concrete unit frames, and the bracing members were attached indirectly to the RC frame via these steel frames (Ohishi et al. 1988; Hjelmstad et al. 1988; Tagawa et al. 1992). In the direct connection method, on the other hand, the steel braces are directly connected to the RC frames without the use of the intermediary steel frame and with the aid of a gusset plate and connecting plates.

Both the external bracing and the indirect internal bracing systems, developed primarily as retrofitting measures, have some drawbacks including architectural limitations, cost and technical difficulties in attaching the brace system to the concrete frame. These considerations make

Springer

the two systems less attractive compared to the directly connected internal bracing.

The direct internal bracing can be used not only as a retrofitting system for existing buildings, but also as a shear-resisting element to be used in the seismic design of new buildings. Experimental and theoretical studies conducted by Maheri et al. (1997, 2003), Maheri and Akbari (2003), Ghaffarzadeh and Maheri (2006), Maheri and Ghaffarzadeh (2008), Tasnimi and Massomi (1999) and Abou-Elfath and Ghobarah (2000) have shown that by using appropriate forms of direct internal bracing, it is possible to enhance load-resisting capacity of RC frames and to improve their seismic performance.

The effectiveness of the brace–RC frame system in resisting loads depends, to a large extent, on the effectiveness of the connections between the two systems in transferring loads. Maheri and Hadjipour (2003) proposed some connection types for retrofitting cases as well as for new constructions. They designed three types of connections combining the current provisions for designing brace–frame connections in steel frames (AISC 2001) and base plate–concrete foundation connections (ACI Committee 318 2002). They constructed full-scale specimens and tested them to ultimate failure of the brace member under direct tensile loads. The force–displacement response of the tested connections indicated their ability to transfer loads between the connected systems. In that study, the authors reported only on the results of static direct tensile tests of the three connection specimens and showed that connections can be designed and constructed so that successful transfer of loads between the brace and concrete members can be achieved up to failure of the brace member. No attempts were made to evaluate the response numerically and to compare the performance of the three connections.

In the present study, results of tests carried out by Maheri and Hadjipour (2003) are first used to calibrate numerical models developed for the three connection types presented. Numerical models of brace–RC frame systems connected using the three types of connections are then developed and analysed under cyclic loading. The results, in the form of hysteresis loops, are subsequently used to evaluate strength and performance parameters of the frames so that appropriate comparisons could be made between the three connections.

2 Experimental Results

The three connection specimens tested by Maheri and Hadjipour are as follows:

Connection type (a) This connection is a typical corner connection for X-bracing. The dimensions and details of the specimen for this connection type are illustrated in Fig. 1a. In this connection, the connecting plates are fixed to the concrete members through hooked anchor bolts embedded in concrete. The connection is therefore suitable for new construction.

Connection type (b) This connection type is identical to type (a), except for the method of fixing the connecting plates to the concrete members. The plates are fixed to the concrete members using straight bolts, anchored at the opposite face of the member by a back plate. The connection is most suited for retrofitting of existing RC frames. It can also be used in new constructions. The details of the connection type (b) are shown in Fig. 1b.

Connection type (c) This connection is designed to increase ductility of the braced frame. It is similar, in principle, to knee bracing, with the single connecting plate replacing the knee element. This connection type requires special provisions at the concrete beam–column intersection as shown in Fig. 1c. The corner of the frame is built-up with concrete so that only one connecting plate is used to transfer the brace load through the joint. The performance of the connection is governed by the response of this single connecting plate.

The full-scale RC frame members and the brace member used for the three connection specimens were identical so that differences could be directed at the connections alone. The steel sections used for braces were ST37 steel angles ($f_y = 240$ MPa), and the concrete had a minimum compressive strength, $f_c' = 41$ MPa (Maheri and Hadjipour 2003). To be able to apply direct tension to the connections through the brace, a 20-mm-thick reaction plate was anchored to the purposely prepared opposite corner of the connections by using four 25-mm-diameter bars. A 100-t capacity universal loading apparatus was used to conduct the direct tensile tests on the connections. A number of mechanical strain gauges were positioned on the connections so that the displacements of the main connection members including the brace, gusset and connecting plates could be recorded. Figure 2 shows the positions of the measuring gauges, denoted by L_1, L_2 and L_3, measuring elongation of the brace, displacement on the gusset and displacement on the connecting plate–concrete arm, respectively.

The results of the direct tensile test on the connections in the form of force–displacement curves are shown in Figs. 3, 4 and 5 for connection types (a) to (c), respectively.

3 Numerical Modelling

In this study, the ANSYS finite element software (ANSYS 2009) was used for the nonlinear numerical analyses of the models. All physical elements within the RC frame, the

Fig. 1 Details of connection specimen types (a), (b) and (c) constructed for direct tensile test (Maheri and Hadjipour 2003)
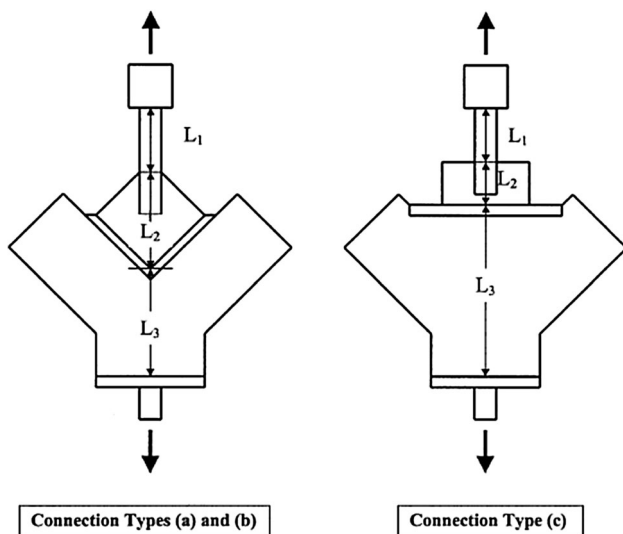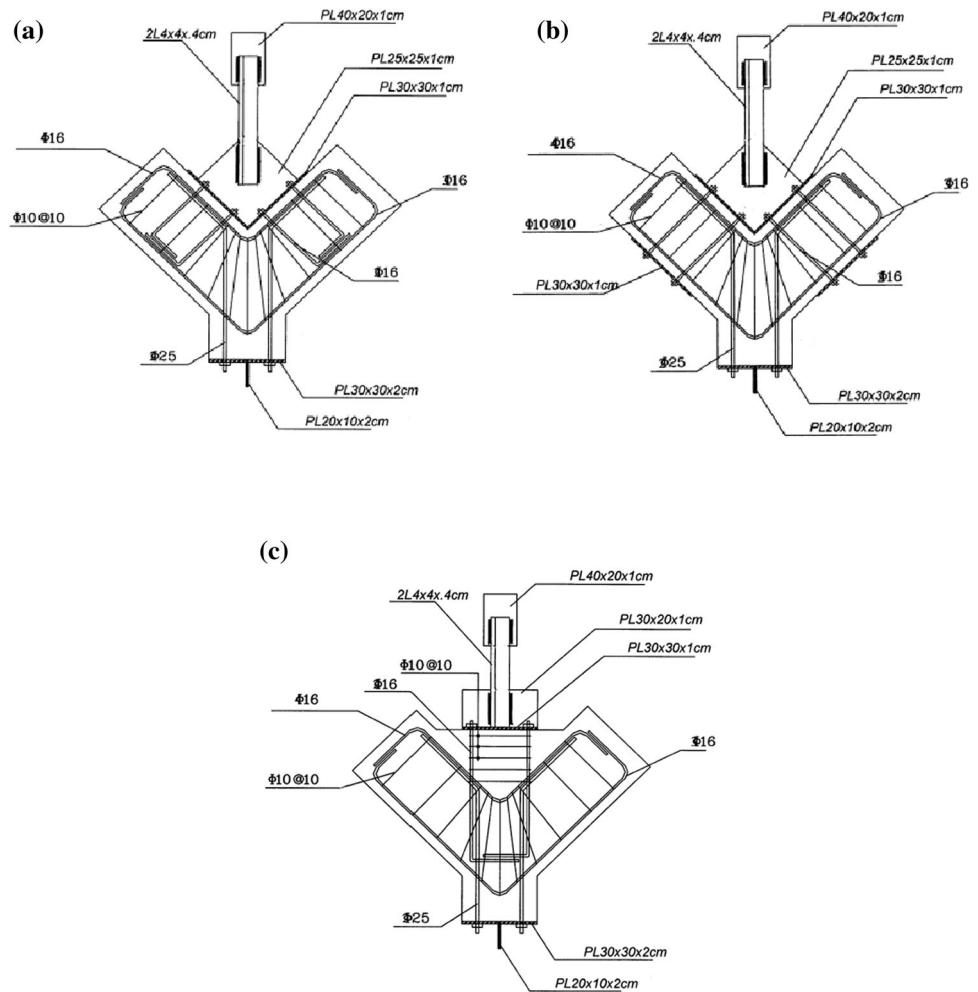

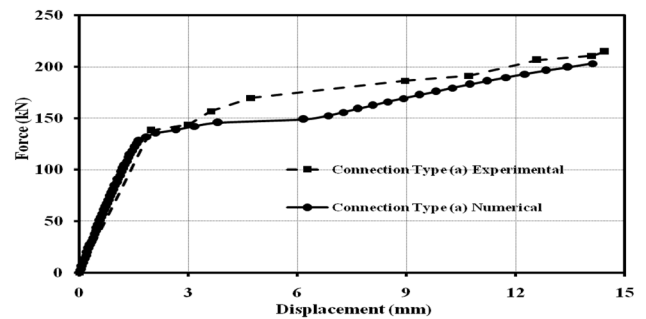**Fig. 2** Position of displacement gauges during tests on connections (Maheri and Hadjipour 2003)

Fig. 3 Force–displacement curves for connection type (a)

bracing system and the brace–frame connections, including the steel reinforcements, were modelled individually for increased accuracy. Three types of elements were used to model the connection specimens: SOLID65 elements were used for concrete; SOLID45 elements were utilised to model the steel bracings, gusset plates, and the connection
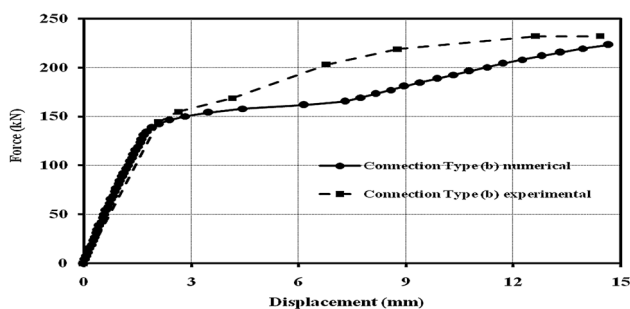
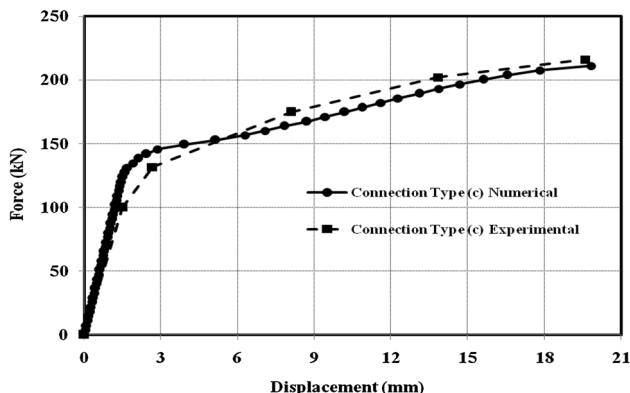**Fig. 4** Force–displacement curves for connection type (b)

Fig. 5 Force–displacement curves for connection type (c)

plates; and LINK8 elements were used to model reinforcements and the anchor bars. The finite element numerical model of the full-scale connection type (a) is shown in Fig. 6. The boundary conditions of each model and the loading procedures were set to represent, as accurately as possible, the actual test condition for that model.

In ANSYS software, the SOLID65 element is specifically developed for concrete materials. This element is capable of handling plasticity, creep, cracking in tension and crushing in compression. In this study, the shear transfer indices in open cracks (β_t) and close cracks (β_c)

were selected as 0.25 and 0.75, respectively, based on suggestions made by Kachlakev et al. (2001). Also, the Hognestad model was used to represent the concrete material stress–strain relation (ANSYS 2009). The SOLID65 elements representing concrete were also allowed to undergo large deformations; however, the limiting strain for concrete failure was considered to be 0.003.

SOLID45 elements were used to model the steel elements. All constant quantities chosen for this element were the software's default values. However, the hourglass check was activated to improve the rate of convergence (ANSYS 2009). Also, the Park model was used to model the reinforcement behaviour (Park and Mander 1984), and the Holzer mathematical model (1975) was utilised to represent the behaviour of steel used in brace elements and the gusset and connecting plates. The material properties used in the numerical analyses of different connections are those reported in references (Maheri and Hadjipour 2003). To perform the nonlinear analyses, the load was applied step by step and the modified Newton–Raphson method was used for the solution.

4 Verification of the Numerical Models

In order for the accuracy of the numerical models to be verified, in this section the results of numerical analyses carried out on the aforementioned models are compared with the results deduced from the experiments. The force–displacement response curves for the full-scale corner connection types (a), (b) and (c) obtained from the experiments are shown in Figs. 3, 4 and 5. These connection models were also analysed numerically, and the corresponding results are presented in the same figures for comparison with those of the experiments. Figure 3 compares the overall response curve for type (a) connection. Close agreement can be seen between the numerical and experimental response curves. Similarly, the numerical response curve of connection type
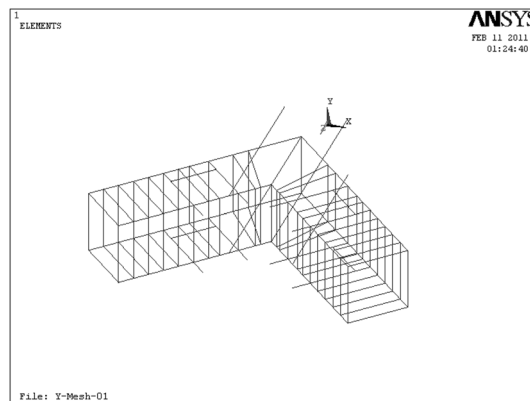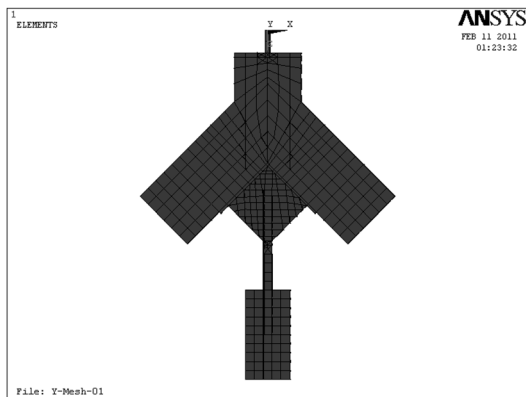

Fig. 6 Meshing of the connection type (a) specimen

Fig. 7 Force–displacement curves for different parts of connection type (a)

Fig. 8 Force–displacement curves for different parts of connection type (b)
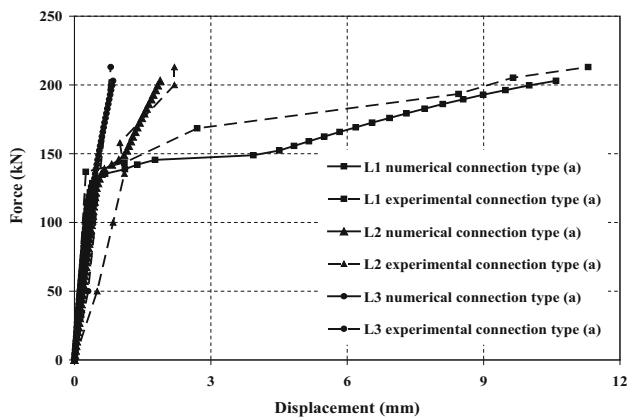

Fig. 9 Force–displacement curves for different parts of connection type (c)

(b) can be seen in Fig. 4 to be close to the experimental curve. The closeness of the force–displacement response curve obtained from the numerical model of the connection type (c) to that obtained from the experiment, as shown in Fig. 5, indicates the accuracy of the numerical model and the method of analysis.

It is a well-known fact that FE-based numerical models generally produce upper-bound solutions to stress analysis problems. In Figs. 3, 4 and 5, it is evident that the numerical model is expectedly slightly stiffer than the experimental models prior to yielding. However, the complex nature of the connections consisting of a number of different interacting parts has resulted in the experimental data slightly deviating from the general trend after the yield point. Nevertheless, numerical and experimental results at ultimate strength become very close again in all three connection types.

In order for the response of different parts of the corner connections to be studied, experimental responses of the three parts of the connections, namely parts L_1, L_2 and L_3, introduced in Fig. 2, are separately shown in Figs. 7, 8 and 9 for connection types (a) to (c), respectively. The numerical responses for the same three sections of each connection type are also extracted from the numerical analyses and are shown for comparison with the experimental results in the same figures.

Regarding the connection type (a), it is evident in Fig. 7 that prior to yielding of brace member, all three sections of the connection including the brace member, the gusset plate and the reinforced concrete corner actively contribute to the response; all three sections show almost linear responses. Since the connection was designed and detailed so that the brace member would yield prior to the gusset plate, connecting plates and the anchor rods, such behaviour was expected. However, after yielding of the brace member, the section relating to this member dominates the response of the connection assembly until the rupture of the
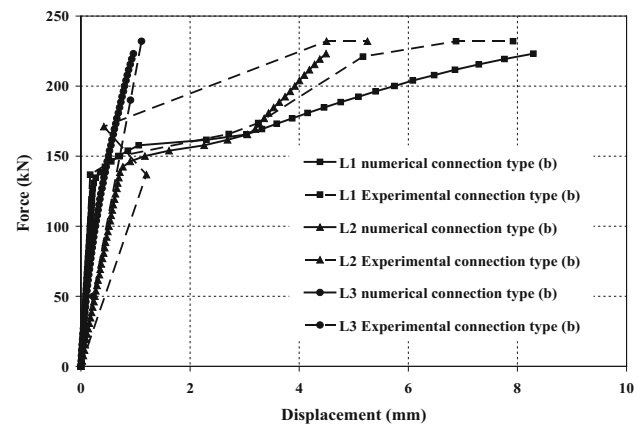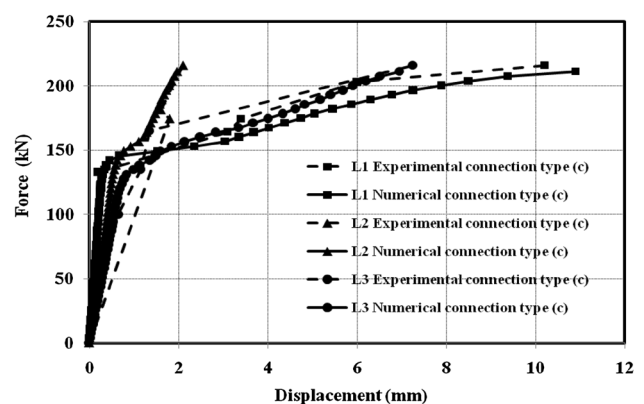
brace. Similar behaviour can be noted for connection type (b) shown in Fig. 8. In connection type (c), relative responses of the three parts of the connection are initially similar to those of connection types (a) and (b). However, yielding of the connection plate prior to yielding of the brace member differentiates the response of this connection at higher loads. As it can be noted in Fig. 9, yielding of the connecting plate is followed by yielding of the brace member. This figure shows that, unlike connection types (a) and (b), after yielding of the brace member, the response of the connection is dominated by both the connecting plate and the brace member in their nonlinear zones while the gusset plate remains elastic.

5 Seismic Performance Parameters of Frames with the Three Connection Types

Seismic performance of a system may be judged by certain parameters including lateral capacity, stiffness, energy dissipation capacity and ductility. Robust seismic

🌳 Shiraz University   ② Springer

performance is due to systems which can undergo large inelastic displacements without much reduction in strength and stiffness. High strength and stiffness, together with high ductility, produce systems which can sustain and dissipate large amounts of energy. Since the only differences in the three types of connections discussed earlier are due to the details of connections, a comparison between different seismic parameters of these connections can highlight the possible efficiency of the connection types. In the following, parameters such as capacity, stiffness, stiffness degradation, energy dissipation, equivalent damping ratio and ductility ratio for the three connection types are computed and compared. For this purpose, and so that the performance of different connections within a complete brace–RC frame system could be judged, full-scale models of a unit RC frame are considered. The full-scale RC frame chosen for this purpose is a unit frame considered previously by Ghaffarzadeh and Maheri (2006) and Maheri and Ghaffarzadeh (2008). Details of the full frame including the material properties are given in (Ghaffarzadeh and Maheri 2006). The same assumptions, parameters and types of elements as those used in the numerical models of the individual connections are used for the full brace–frame systems. Also, details of the connections were assumed to be the same as those discussed previously for the connection specimens alone. Three brace–frame models, each having a different connection type [(a), (b) or (c)], were created and subjected to nonlinear in-plane pushover analyses. The numerical model of the brace–RC frame system connected together with the connection type (a) is shown in Fig. 10.

Nonlinear cyclic analysis was performed on the numerical model of each frame. The steps and details of the cyclic analyses are the same as those used in Ghaffarzadeh and Maheri (2006). Figure 11 shows the hysteresis loops obtained from the cyclic analyses of the three frames.
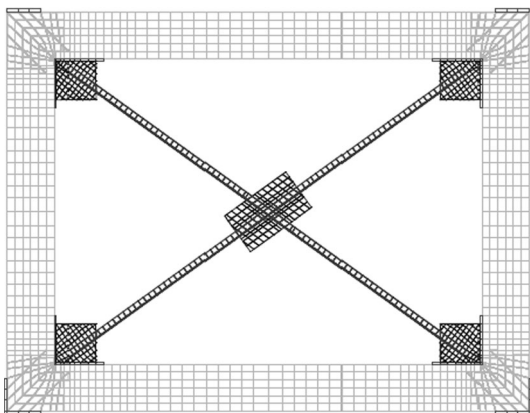

Fig. 10 Numerical model of the brace–frame system with connection type (a)

It can be seen in Fig. 11 that the response of the connection types (a) and (b) in terms of stiffness, capacity and energy dissipation is relatively similar. This was expected as the two types of connections are inherently similar in form. However, the connection type (c) shows fatter loops, indicating a larger energy dissipation capacity. These parameters are further discussed and compared as follows.

5.1 Strength Capacity

So that some performance parameters, including the strength capacity, could be calculated from the results of analyses, the maximums of the hysteresis loops for each frame are determined and plotted as response curves in Fig. 12. The strength capacity of the frames can be deduced from these curves. As it can be seen in this figure, the strength capacity of the frame with connection type (b) is somewhat more than that of connection types (a) and (c). However, the small differences in strength capacities of the frames with the three connection types indicate that all three connections are equally capable of sustaining loads and providing the necessary lateral resistance.

5.2 Stiffness and Stiffness Degradation

The average lateral stiffness of a system during a cycle of loading can be evaluated as the slope of the line joining the maximum positive and negative points in that loop. Stiffness of each brace–frame system during different loading cycles was determined as shown in Fig. 13. This figure shows degradation of stiffness as a function of the lateral drift of the braced frame. A number of factors may contribute to stiffness degradation in an RC frame; these include bond degradation, concrete stiffness degradation due to the development of micro-cracks and Boushinger effects in reinforcements. In a braced frame, other factors such as stiffness degradation in connection elements, particularly in the connecting plates and anchor bolts, also contribute to the overall response. This point can be seen when we compare the stiffness degradation in the frame with connection type (a) with that of the frame of connection type (b). The only difference between these two frames is the method in which the anchor bolts are fixed to the concrete members; in connection type (b), the anchoring arrangement results in a stiffer and more robust connection. The marked reduction in the stiffness of the frame with type (c) connection compared to the other two frames is evidently due to the flexible response of the single connection plate in bending. Figure 13 also shows that the initial stiffness of the frame with type (c) connection is much less than the initial stiffness of the frames with the other two connection types. The values of stiffness of the three frames, however, become closer at higher levels of lateral
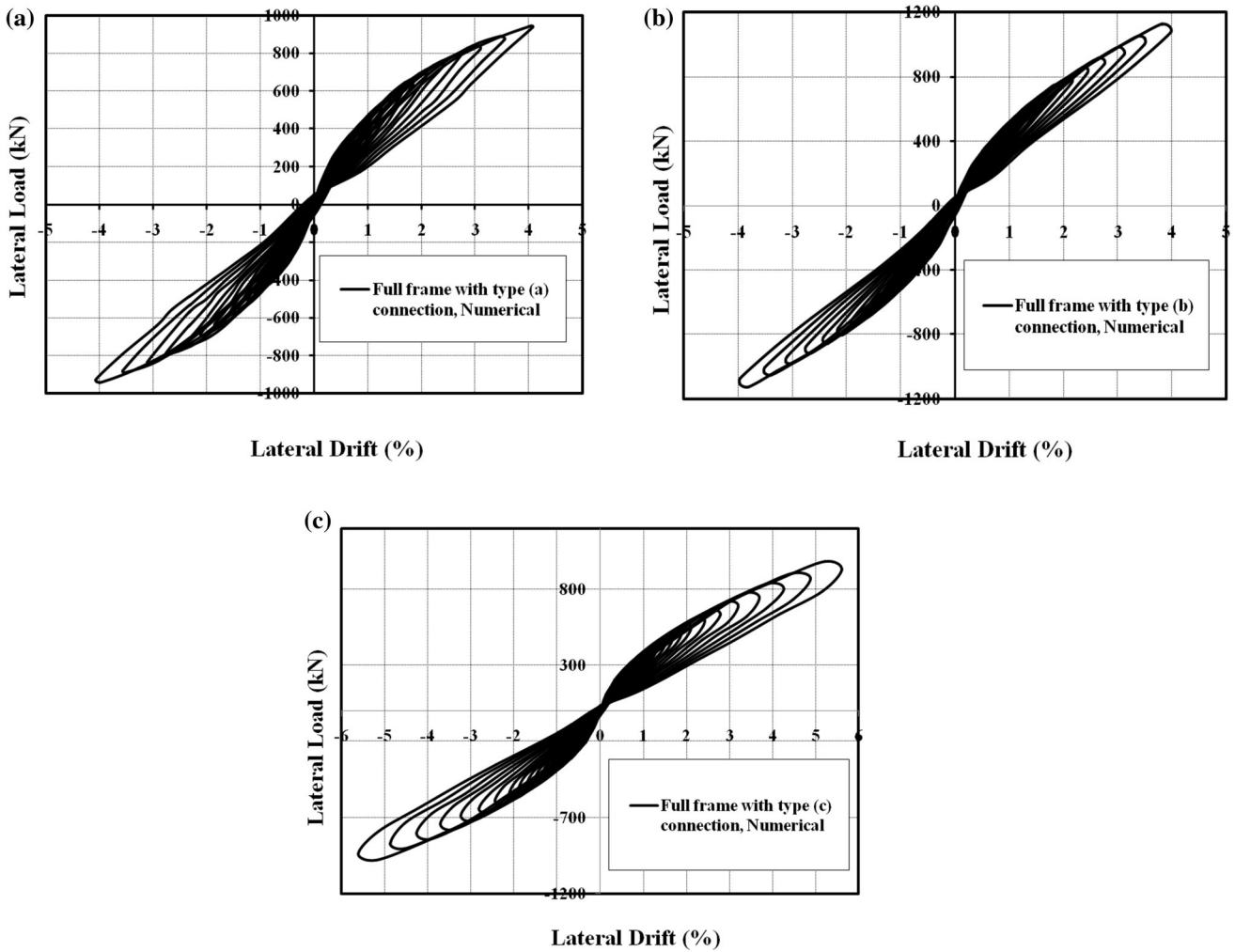
Fig. 11 Response hysteresis loops for brace–frame systems with connection types (a), (b) and (c)
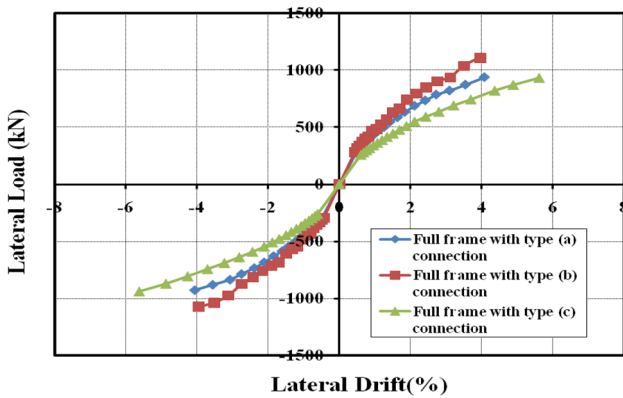

Fig. 12 Comparison between the maximum and minimum values of hysteresis loops for frames with different brace–frame connections
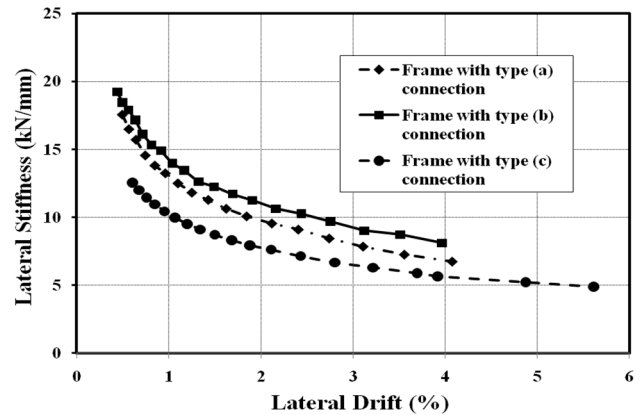

Fig. 13 Stiffness degradation in the three frames with different brace–frame connections

drift. This indicates a lower rate of stiffness degradation for type (c) connection compared to the other two connections. The better performance of type (c) connection in this regard is further evident when we note that the brace–frame with

connection type (c) is capable of undergoing much larger lateral drifts (around 40 % higher) than the brace–frame systems with connection types (a) and (b).
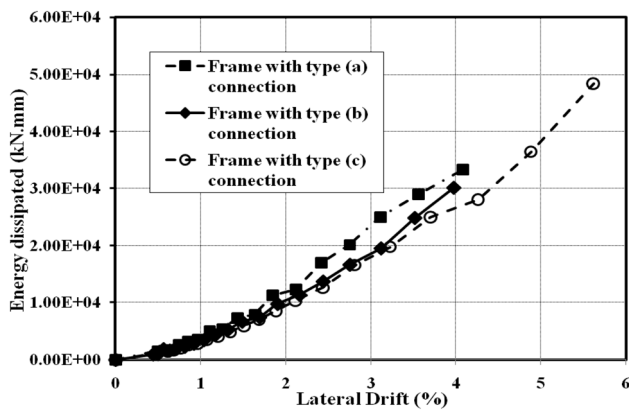
Fig. 14 Energy dissipation in the three frames with different brace–frame connections

Fig. 15 Equivalent damping ratio for frames with different brace–frame connections

5.3 Energy Dissipation Capacity

The ability to dissipate energy is an advantageous capacity for systems undergoing seismic loading. This capacity, also termed 'toughness', is measured as the area under the force–deformation curve. For the three brace–frame systems, the energy dissipated in each cycle of loading was calculated. The cumulative energy dissipated by the three brace–frame systems is plotted as a function of lateral drift in Fig. 14. This figure indicates that the brace–frame systems with type (a) and type (b) connections have more or less similar energy dissipation capacities, whereas the frame with connection type (c) exhibits a much larger energy dissipation capacity (around 60 % more).

5.4 Equivalent Damping Ratio

The energy dissipation capacity may also be evaluated in terms of the equivalent damping ratio. The equivalent damping ratio, ξ_{eq}, may be evaluated as follows:

$$\xi_{eq} = \frac{1}{4\pi} \frac{E}{E_{so}} \tag{1}$$

where E is the energy dissipated in one cycle and E_{so} is the strain energy. This parameter is also calculated for the three brace–frame systems and is plotted as a function of the lateral relative drift in Fig. 15. It can be seen that for each frame, this parameter fluctuates around a certain mean value which can be considered as the value of the equivalent damping ratio for that frame. Comparing the values of this parameter for the three brace–frame systems reveals that the systems with connection types (a) and (c) exhibit higher damping ratios compared to frame with type (b) connection. Energy dissipation due to inelastic response of the single connecting plate in type (c) connection and the bond degradation in the anchor bar–concrete assembly
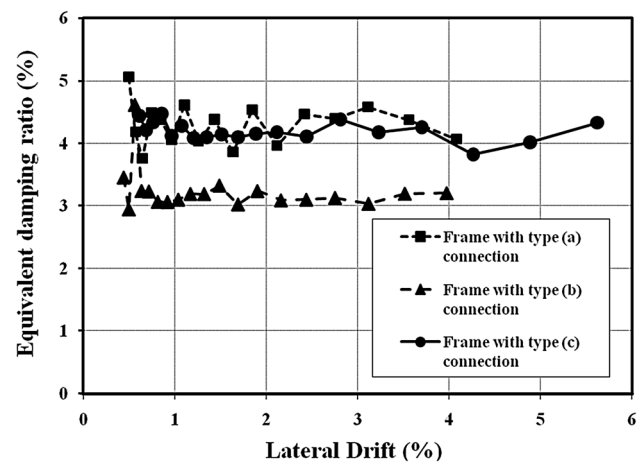
in type (a) connection may be considered as explanations for the differences in these values.

5.5 Ductility Ratio

Ductility is one of the most important parameters affecting the seismic performance of a structure. In a frame, ductility ratio, μ, is defined as the ratio of the ultimate (or a pre-specified maximum) lateral displacement at roof level Δ_{max} (i.e. drift) to the displacement at the equivalent yield point of the frame Δ_y. With reference to Fig. 16, the equivalent yield point is determined by introducing a bilinear representation of the response curve, having the same area under the force–displacement curve as the actual response curve. The response curve is best obtained through a nonlinear pushover analysis of the system to failure. In cases where nonlinear cyclic analysis is carried out, the response curve may be considered as the line joining the maximum points of the hysteresis loops in the positive zone. The response curves for the brace–frame systems having connection types (a), (b) and (c) are plotted in Fig. 16a–c, respectively. Different approaches may be used to model the response curve by a bilinear curve. In this study, two approaches are used: (i) initial stiffness is considered as the slope of the first line, and (ii) the secant stiffness at 60 % of total capacity is assumed to represent the first line. A horizontal line is considered in both approaches to represent the second line.

The values of ductility ratio, μ, evaluated for the three brace–frame systems using the two approaches are compared graphically in Fig. 17. The frames with type (a) and type (c) connections show higher ductility ratios compared to the frame type (b). This is in line with the results obtained for the equivalent damping ratio; however, the parity of ductility for connection types (a) and (c) is rather
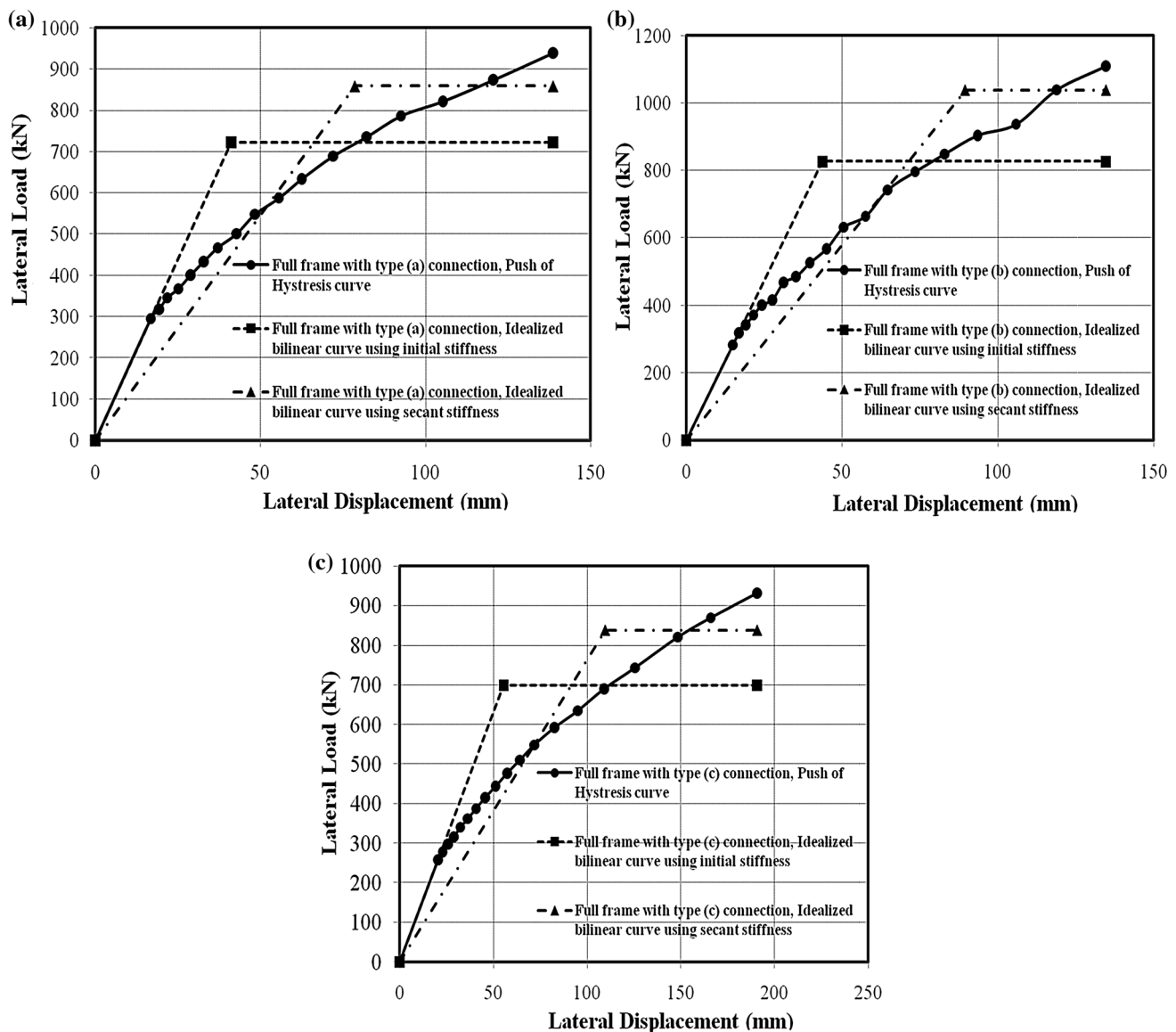
Fig. 16 Different bilinear representations of the response curves for evaluation of damping ratio

surprising; as in other seismic performance parameters, including the stiffness degradation and the energy dissipation capacity, type (c) connection appears markedly superior. The parity of the ductility ratios for types (a) and (c) as evaluated here may be due to the types of bilinear representation of the response curve selected. Other representations may produce more marked differences.

6 Conclusions

Results of the numerical investigation carried out in this paper on evaluating the seismic performance parameters of steel bracing and RC frames connected together using three different connection types may be summarised as follows:

1. All three connections types showed sufficient robustness in transferring loads between the brace system and the RC frame.
2. The connection type (b), in which drag-through anchor bolts fix the connecting plates to back plates, appeared to be more robust in terms of strength and stiffness compared to the other two connection types. However, it showed inferior seismic performance regarding energy dissipation capacity and ductility.
3. Compared to connection type (b), the connection type (a) appeared to be a safer design in terms of energy dissipation and ductility; however, they lack the capacity of connection type (c) in these regards.
4. The new, built-in connection type (c) in which brace load is directly transferred to the concrete frame
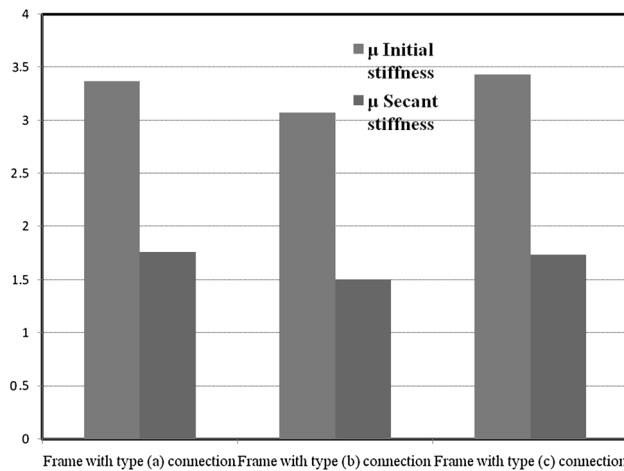
Fig. 17 Ductility ratios evaluated using the initial stiffness and the secant stiffness methods

through a single connecting plate showed the best performance in terms of stiffness degradation, energy dissipation capacity, damping ratio and ductility. Its performance may be likened to eccentric knee-braced systems, the connecting plate acting as a knee element. Further work is needed to evaluate the performance of this innovative connection and provide design basis for such connections.

References

Abou-Elfath A, Ghobarah A (2000) Behaviour of reinforced concrete frames rehabilitated with concentric steel bracing. Can J Civ Eng 27:433–444

ACI Committee 318 (2002) Building code requirements for reinforced concrete (ACI 318-02) and commentary (ACI 318R-02). American Concrete Institute, Detroit, Michigan

AISC (2001) Manual of steel construction: load and resistance factor design, 3rd edn. American Institute of Steel Construction, Chicago

ANSYS (2009) ANSYS user's manual, revision 12. ANSYS Inc, Canonsburg, Pennsylvania

Badoux M, Jirsa JO (1990) Steel bracing of RC frames for seismic retrofitting. J Struct Eng ASCE 116(1):55–74

Bush TD, Jones EA, Jirsa JO (1991) Behavior of RC frame strengthened using structural-steel bracing. J Struct Eng ASCE 117(4):1115–1126

Ghaffarzadeh H, Maheri MR (2006) Cyclic tests on the internally braced RC frames. JSEE 8(3):177

Hjelmstad KD, Fooooooutch DA, Del Valle E, Downs RE (1988) Forced vibration studies of an RC building retrofit with steel bracing. In: Proceedings of 9th world conference on earthquake engineering, Japan, VII, pp 469–474

Holzer S (1975) SINDER: a computer code for general analysis of two-dimensional reinforced concrete structures. Report. AFWL-TR-74-228 vol 1. Air force Weapons Laboratory, Kirt-Land, AFB, New Mexico

Kachlakev D, Miller T, Yim S, Chansawat K (2001) Finite element modeling of reinforced concrete structures strengthened with FRP laminates. Final report for Oregon Department of Transportation Research Group

Maheri MR, Akbari R (2003) Seismic behaviour factor, R, for steel X-braced and knee-braced RC buildings. Eng Struct 25(12):1505–1513

Maheri MR, Ghaffarzadeh H (2008) Connection overstrength in steel-braced RC frames. Eng Struct 30(7):1938–1948

Maheri MR, Hadjipour A (2003) Experimental investigation and design of steel brace connection to RC frame. Eng Struct 25:1707–1714

Maheri MR, Sahebi A (1997) Use of steel bracing in reinforced concrete frames. Eng Struct 19(12):1018–1024

Maheri MR, Kousari R, Razazan M (2003) Pushover tests on steel X-braced and knee-braced RC frames. Eng Struct 25(13):1697–1705

Ohishi H, Takahashi M, Yamazaki Y (1988) A seismic strengthening design and practice of an existing reinforced concrete school building in Shizuoka city. In: Proceedings of 9th world conference on earthquake engineering, Japan, VII, pp 415–420

Park R, Mander JB (1984) Theoretical stress-strain model for confined concrete. ASCE J Struct Eng 114:1804–1826

Tagawa Y, Aoki H, Huang T, Masuda H (1992) Experimental study of new seismic strengthening method for existing RC structure. In: Proceedings of 10th world conference on earthquake engineering, Rotterdam, pp 5193–5198

Tasnimi A, Masoomi A (1999) Evaluation of response of reinforced concrete frames strengthened with steel bracing. In: Proceedings of the third international conference on seismology and earthquake engineering, Iran